

Native State Volume Fluctuations in Proteins as a Mechanism for Dynamic Allostery

Anthony B. Law,[†] Paul J. Sapienza,[‡] Jun Zhang,[§] Xiaobing Zuo,[⊥] and Chad M. Petit^{*,||}

[†]Department of Otolaryngology – Head and Neck Surgery, University of Washington, Seattle, Washington 98195, United States

[‡]Division of Chemical Biology and Medicinal Chemistry, UNC Eshelman School of Pharmacy, University of North Carolina at Chapel Hill, Chapel Hill, North Carolina 27599, United States

[§]Department of Chemistry, University of Alabama at Birmingham, Birmingham, Alabama 35294, United States

[⊥]X-ray Science Division, Argonne National Laboratory, Argonne, Illinois 60439, United States

^{||}Department of Biochemistry and Molecular Genetics, University of Alabama at Birmingham, Birmingham, Alabama 35294, United States

Supporting Information

ABSTRACT: Allostery enables tight regulation of protein function in the cellular environment. Although existing models of allostery are firmly rooted in the current structure–function paradigm, the mechanistic basis for allostery in the absence of structural change remains unclear. In this study, we show that a typical globular protein is able to undergo significant changes in volume under native conditions while exhibiting no additional changes in protein structure. These native state volume fluctuations were found to correlate with changes in internal motions that were previously recognized as a source of allosteric entropy. This finding offers a novel mechanistic basis for allostery in the absence of canonical structural change. The unexpected observation that function can be derived from expanded, low density protein states has broad implications for our understanding of allostery and suggests that the general concept of the native state be expanded to allow for more variable physical dimensions with looser packing.

Proteins are classically viewed to fold into a single conformation defined by the close-packing of its constituent atoms.¹ From X-ray crystallography, the packing of protein interiors has been found to be remarkably uniform, with the fraction of occupied space lying in the narrow range of 0.74 ± 0.02 .^{2–4} The idea that proteins must pack as efficiently as organic crystals is contrasted by the discovery that a significant fraction of proteins do not fold and indeed function as a consequence of their intrinsic structural disorder.⁵ These two extremes define an order–disorder continuum within which any point, in principle, can represent the preferred degree of order for a given protein sequence (Figure 1). As an example, a subset of proteins known as “molten globules” occupies a reasonably well-defined segment of the order–disorder continuum distinct from classically native proteins.⁶ If both compact (native) and expanded (molten globule) states of proteins can stably exist, it is not clear why additional intermediate states cannot.

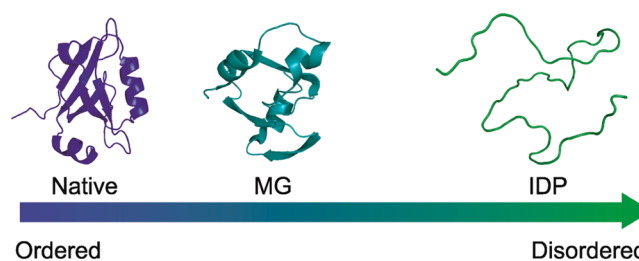


Figure 1. Order–disorder continuum. Graphic representation of the order–disorder continuum with known states that proteins can adopt indicated above.

Previously, we found that undocking of a C-terminal helical extension ($\alpha 3$) of the third PDZ domain (PDZ3) from the neuronal scaffolding protein postsynaptic density-95 (PSD-95) causes significant, nonlocalized increases in side-chain mobility on the picosecond–nanosecond (ps–ns) time scale.⁷ This undocking occurs naturally upon phosphorylation of Y397 located in the helical extension which, in turn, allosterically regulates binding to the PDZ ligand CRIPT.^{7,8} We concluded that distal modulation of the binding function PDZ3 occurs via a delocalized, conformational entropy based mechanism. This mechanism is facilitated by the increased side-chain mobility observed in the undocked $\alpha 3$ variant of PDZ3 and is independent of gross structural change. Indeed, the concept of using ps–ns side-chain motions as a proxy for conformational entropy was highlighted in a recent review by Wand.⁹ Although it is clear from this review that ps–ns side-chain dynamics scale underlie the entropic contribution to protein function in many systems, the determinant of these motions is still unclear as they do not correlate with depth of burial, packing density from deposited coordinates, or degree of surface exposure.¹⁰

Given the general interest in the determinant of ps–ns side-chain motions, we set out to investigate the underlying mechanism of the dynamic phenomenon observed in our previous study⁷ through an extensive combination of

Received: November 22, 2016

Published: January 17, 2017

biophysical experiments. The same two constructs of PDZ3 were used as in the previous study for this biophysical characterization: the “canonical” PDZ3 in which the C-terminus occurs at position 402 (PDZ3⁴⁰²) and thereby contains $\alpha 3$;¹¹ and a truncated PDZ3 which is a mimic of PDZ3 phosphorylated at Y397,^{7,8} referred to herein as PDZ3^{P($\Delta\alpha 3$)}. One peculiar observation from our previous study that we felt may shed light into the enhanced side-chain motions of PDZ3^{P($\Delta\alpha 3$)} concerned the values of the overall rotational correlation times (τ_m) for both proteins. Given that the value of τ_m correlates with molecular weight, it was expected, *a priori*, that PDZ3^{P($\Delta\alpha 3$)} would have a lower τ_m than PDZ3⁴⁰². However, the τ_m values determined from ¹⁵N spin-relaxation experiments were almost identical (τ_m of 6.0 and 5.9 ns for PDZ3^{P($\Delta\alpha 3$)} and PDZ3⁴⁰², respectively).⁷ This indicates that both proteins have the same tumbling time despite a 10% reduction in molecular weight of PDZ3^{P($\Delta\alpha 3$)} when compared to PDZ3⁴⁰². From this observation, we hypothesized that topological differences between the two proteins may give rise to the larger than expected τ_m of PDZ3^{P($\Delta\alpha 3$)}.

To test this hypothesis, we performed a battery of biophysical experiments to evaluate topological differences between the two proteins. The HSQC spectra of both proteins show excellent chemical shift dispersion indicative of highly structured, stable proteins (Figure S1A,B). Truncating the $\alpha 3$ helix has a negligible effect on the structure of PDZ3⁴⁰² as demonstrated by chemical shift perturbation⁷ and NOESY analysis (Figure S2). Consistent with these observations, both PDZ3 constructs display standard two-state cooperative unfolding, with PDZ3^{P($\Delta\alpha 3$)} being modestly less stable ($\Delta G_{\text{unf}} = 4.7 \text{ kcal mol}^{-1}$) when compared to PDZ3⁴⁰² ($\Delta G_{\text{unf}} = 6.6 \text{ kcal mol}^{-1}$) (Figure S1C). This is further supported by differential scanning calorimetry (DSC) isotherms, which show stable pretransition baselines up to 42 and 55 °C for PDZ3^{P($\Delta\alpha 3$)} and PDZ3⁴⁰², respectively (Figure S1D). Collectively, these data show that both PDZ3 constructs have identical topology. They also strongly indicate that both constructs are not molten globules and that solvent has not penetrated into the core of either protein; rather, they are natively folded under all conditions used in the subsequent experiments.

Although the NOE patterns are virtually identical between the two proteins, the NOE peaks are systematically weaker for PDZ3^{P($\Delta\alpha 3$)} by ~17% (Figure 2A and S2). Because there is no evidence of conformational exchange on the μs – ms time scale, we conclude that the systematic weakening of the NOE peaks arises from greater distances, on average, between the atoms (Figure S2, see Supplemental Discussion (SD) 1). Therefore, we assessed the overall size and shape of each protein using small-angle X-ray scattering (SAXS). Surprisingly, the radius of gyration (R_g) of PDZ3^{P($\Delta\alpha 3$)} was larger at 15.9 Å than PDZ3⁴⁰² (14.7 Å), even though it contains seven fewer residues (Figure 2B). This is consistent with the overall rotational correlation times determined from ¹⁵N spin relaxation experiments.⁷ We previously observed that binding of PDZ3 ligand (C-terminal peptide from CRIPT) returned the unusually flexible side-chain dynamics in PDZ3^{P($\Delta\alpha 3$)} back to the levels observed in PDZ3⁴⁰².⁷ Similarly, the PDZ3^{P($\Delta\alpha 3$)}.CRIPT complex showed a reduced R_g of 13.6 Å, despite addition of the peptide (Figure 2B). Thus, the binding of peptide ligand reduced the overall radius (and by extrapolation, volume) of PDZ3^{P($\Delta\alpha 3$)}. A more subtle reduction in R_g of 0.4 Å was observed for PDZ3⁴⁰², indicating that both proteins are made more compact upon the

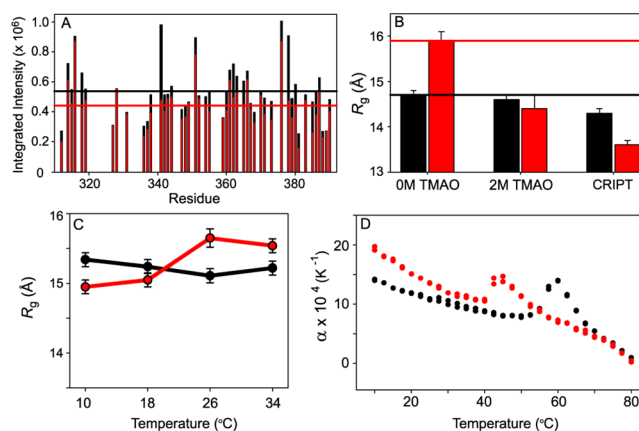


Figure 2. Volumetric differences between PDZ3⁴⁰² and PDZ3^{P($\Delta\alpha 3$)}. For this and all subsequent figures, data associated with PDZ3 will be in black whereas data associated with PDZ3^{P($\Delta\alpha 3$)} will be in red. (A) Integrated intensity of amide and C α NOE crosspeaks to the backbone amide protons indicated (see Methods). Horizontal lines indicate the average intensity for both proteins. (B) Radii of gyration as determined by SAXS for the apo form, the apo form in the presence of 2 M TMAO, and CRIPT bound. The black and red horizontal lines indicate R_g values for the apo forms of PDZ3⁴⁰² and PDZ3^{P($\Delta\alpha 3$)}, respectively. The reported R_g values are from samples with a protein concentration of 2 mg mL⁻¹ (see Table S1). (C) Radii of gyration as determined by SAXS for the temperatures indicated. (D) Temperature dependence of the coefficient of thermal expansion for both proteins.

addition of CRIPT. Addition of 2 M trimethylamine N-oxide (TMAO), a stabilizing osmolyte, also reduced the R_g for PDZ3^{P($\Delta\alpha 3$)} (14.4 Å), whereas TMAO had no detectable effect on PDZ3⁴⁰² (Figure 2B). It should be noted that the observed changes in R_g cannot be easily explained by oligomerization effects or partial unfolding, as there was no evidence of such behavior under any of the conditions examined (Figures S3, S4, and Table S1). Collectively, these data suggest that PDZ3^{P($\Delta\alpha 3$)}, despite its reduced mass, occupies a significantly greater volume in solution than PDZ3⁴⁰².

As temperature is known to modulate protein volume,¹² we also measured R_g as a function of temperature. The only significant change in radius observed was for PDZ3^{P($\Delta\alpha 3$)} at lower temperatures, resulting in a decrease in R_g of 0.7 Å upon reducing the temperature from 26 to 10 °C (Figure 2C). To test whether these apparent volume changes as a function of temperature could be detected by alternative means, we used pressure perturbation calorimetry (PPC). PPC is an exceptionally sensitive technique that determines the coefficient of thermal expansion (α), defined as $\frac{1}{V} \frac{\partial V}{\partial T}$, as a function of temperature.¹³ As shown in Figure 2D, values of α for PDZ3^{P($\Delta\alpha 3$)} are significantly higher than for PDZ3⁴⁰² at temperatures below 30 °C. This indicates that over this temperature range, the volume of PDZ3^{P($\Delta\alpha 3$)} increases with temperature more than PDZ3⁴⁰². This is consistent with the reduction in R_g for PDZ3^{P($\Delta\alpha 3$)} relative to PDZ3⁴⁰² at lower temperatures. We were also able to conclude that the differences in α were not due to solvation effects (see SD2).

One predicted consequence of a positive (negative) change in protein volume is that the interior would be more dynamic (rigid) due to differences in packing density. Therefore, we used ²H relaxation experiments to obtain methyl order parameters, S_{axis}^2 , under multiple cosolute and temperature conditions as previously described.⁷ The average S_{axis}^2 ($\langle S_{\text{axis}}^2 \rangle$)

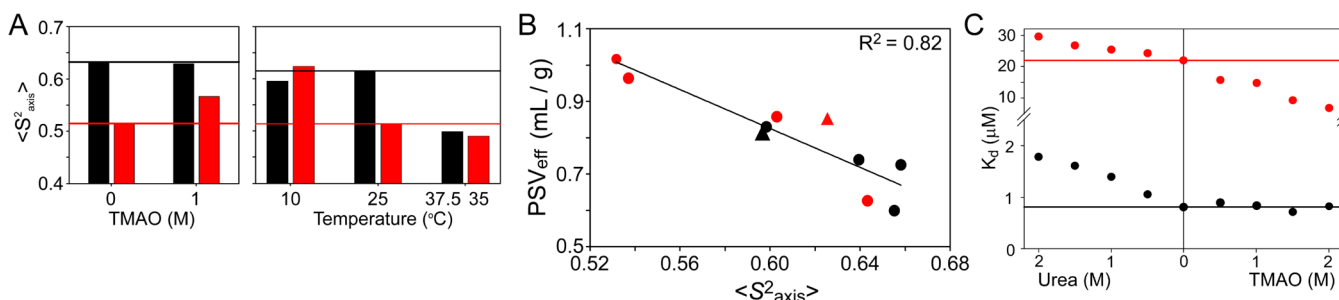


Figure 3. Volumetric effects on side-chain motions and PDZ3 function. (A) Dependence of $\langle S^2_{\text{axis}} \rangle$ on concentration of TMAO and temperature. Black and red horizontal lines indicate $\langle S^2_{\text{axis}} \rangle$ for PDZ3⁴⁰² and PDZ3^{P(Δα3)}, respectively, under reference conditions (0 M TMAO and 25 °C). See Methods for explanation of the slight variation in $\langle S^2_{\text{axis}} \rangle$ for PDZ3⁴⁰². (B) PSV_{eff} was calculated using eq 1 as described in Materials and Methods. The fitted linear correlation coefficient (R^2) of PSV_{eff} versus $\langle S^2_{\text{axis}} \rangle$ is 0.82. Triangles indicate points whose $\langle S^2_{\text{axis}} \rangle$ are linearly extrapolated from measured data to match the conditions of its associated PSV_{eff} (Materials and Methods). If omitted from the plot, R^2 increases to 0.88. (C) Dissociation constant (K_d) as a function of urea and TMAO. Horizontal lines indicate the reference state with no cosolute.

of PDZ3⁴⁰² was largely unaffected by the addition of 1 M TMAO, whereas for PDZ3^{P(Δα3)} it showed significant increase (Figure 3A). This finding is consistent with the observed R_g values for both constructs under similar conditions (Figure 2B). The temperature dependence of side-chain dynamics follows a similar trend. As the temperature is lowered from 25 to 10 °C, there was dramatic rigidification in the side-chain dynamics of PDZ3^{P(Δα3)} whereas PDZ3⁴⁰² showed little effect (Figure 3A).

To fully capture the relationship between side-chain dynamics and interior packing density, we correlated $\langle S^2_{\text{axis}} \rangle$ with an empirically derived protein density parameter termed “effective partial specific volume” (PSV_{eff}). PSV_{eff} approximates the partial specific volume for apo PDZs or CRIPT-bound complexes using R_g values (Materials and Methods). As shown in Figure 3B, there is a linear anticorrelation between $\langle S^2_{\text{axis}} \rangle$ and PSV_{eff}, indicating that as side-chain dynamics increases, overall protein density decreases. This relationship points to a potentially simple determinant of side-chain order parameter values, which do not correlate with depth of burial, packing density from deposited coordinates, or degree of surface exposure.¹⁰ Specifically, S^2_{axis} values would be expected to be low in the context of greater volume (stable or transient) around a residue’s side chain. This coupling of volume and side-chain order parameters adds an intuitive understanding of the dynamic allostery observed previously that utilized side-chain motions as a source of conformational entropy.⁷ Furthermore, the observed relationship between PSV_{eff} and $\langle S^2_{\text{axis}} \rangle$ provides a potential explanation, consistent with Le Châtelier’s principle, of how global motions are coupled to localized motions in the protein interior. This idea is supported by recent work in which high-pressure NMR spectroscopy was used to identify spatially clustered regions within the protein core that have variable compressibilities.¹⁴

To further test this volumetric model, isothermal titration calorimetry (ITC) was used to determine CRIPT peptide binding properties of PDZ3⁴⁰² and PDZ3^{P(Δα3)} as a function of PSV_{eff} (Figure 3C). In addition to TMAO, urea was also used as cosolute as it is widely used to destabilize proteins. In the presence of TMAO, PDZ3^{P(Δα3)} experienced an increase in binding affinity, while PDZ3⁴⁰² was unaffected. The reverse trend was observed over increasing concentrations of urea, with PDZ3⁴⁰² experiencing the more dramatic affinity change when compared to PDZ3^{P(Δα3)}. These changes in binding affinity as a result of volume shifting conditions support a functionally relevant coupling between volume and internal motions. These relationships are summarized in a simple volumetric model that

links changes in protein volume with functional consequences (via conformational entropy), thereby unifying molecular volume, internal dynamics, and protein function (Figure S5). We propose that this volumetric model provides a mechanism for dynamic allostery in the absence of apparent structural change.

Native state volume expansion is not an idiosyncratic feature of this particular domain. A number of X-ray crystallographic studies have revealed temperature dependent changes in lattice contacts, volume, dynamics, core packing, and average structure for a routine set of proteins.^{12,15–17} Recently, exact measurements of NOEs were used to study the temperature dependence of ¹H_N–¹H_N distances in ubiquitin.¹⁸ It was shown that average distance changes of 2.4% (11–34 °C) and 4.0% (11–53 °C) could be detected throughout the protein structure, including α -helical and β -sheet secondary structures. In other work, Gekko and co-workers have demonstrated functionally relevant point mutations that lead to changes in the partial specific adiabatic compressibility ($\bar{\beta}_s^\circ$), a parameter directly linked to volumetric fluctuations.¹⁹ Finally, changes in protein volume upon truncation of ankyrin domain repeats are consistent with the volume effects observed here, though likely not as large.²⁰ We note that although we observe an expansion of PDZ3^{P(Δα3)} to a lower density state relative to PDZ3⁴⁰², the current data are unable to resolve whether this expanded state results from an overall broadening of the distribution of volumes or from a more complete shift of the envelope away from smaller volumes and toward larger volumes. Regardless of the distribution, this expanded state is clearly within the native ensemble and shows that proteins need not form their three-dimensional structures with crystalline-like packing densities.

Although Cooper first argued that proteins undergo sizable fluctuations in volume 35 years ago,²¹ the idea that these fluctuations contribute to protein function is still prevalent today.^{22–25} Here, we present evidence for a stable thermodynamic protein state that is substantially expanded in volume yet displays all the normal characteristics of a tightly packed protein. Such states have hitherto been invisible crystallographically because low temperature data acquisition and cosolvents used as cryoprotectants favor compact states.¹⁷ However, the expanded state was identified here for a PDZ domain using a novel combination of solution based biophysical measurements. Using cosolutes, ligand binding, and temperature, we showed that the protein’s volume is

malleable and correlates with amplitudes of ps–ns side-chain motions. This correlation implicates persistent or transient volume fluctuations as a general determinant of side-chain dynamics within “packed” protein interiors, which has not been well understood.¹⁰ It further suggests that coupling of global volume fluctuations with local side-chain dynamics (a source of entropy) can serve as a mechanism for functional allostery and potentially for additional protein functions, especially for instances in which structural changes are not apparent.²⁶ We stress that all of the routine biophysical measurements of PDZ3^{P(Δα3)} point to traditional two-state folding behavior;^{27,28} however, our data indicate a continuum of volume and dynamic fluctuations within the pretransition region. Although observed only for a PDZ domain here, there is nothing unique or exceptional about the composition of this domain, and hence expanded native states can, in principle, exist for other proteins. This idea is supported by a recent study in which domains in human serum albumin were found to have properties identical to dry molten globules,²⁹ a hypothetical expanded form of native protein structure that shares many characteristics with PDZ3^{P(Δα3)} (see SD3). We conclude that the current definition of the native state, and its associated preconceptions of packing density, may be too narrow for many proteins and may potentially limit our understanding of protein allostery. We propose that the general concept of the native state be expanded to allow for more variable physical dimensions with looser packing.

■ ASSOCIATED CONTENT

Supporting Information

The Supporting Information is available free of charge on the ACS Publications website at DOI: 10.1021/jacs.6b12058.

Supporting figures and discussion as well as detailed experimental procedures (PDF)

■ AUTHOR INFORMATION

Corresponding Author

*cpetit@uab.edu

ORCID

Chad M. Petit: 0000-0003-4933-6245

Notes

The authors declare no competing financial interest.

■ ACKNOWLEDGMENTS

This work was funded by NIH F32GM082006 and UAB institutional funds (C.M.P.) The SAXS measurements were performed at beamline 12-ID-B of Advanced Photon Source at Argonne National Laboratory. This research used resources of the Advanced Photon Source, a U.S. Department of Energy (DOE) Office of Science User Facility operated for the DOE Office of Science by Argonne National Laboratory under Contract No. DE-AC02-06CH11357.

■ REFERENCES

- (1) Fersht, A. *Structure and Mechanism in Protein Science*; W. H. Freeman and Company: New York, 1999.
- (2) Fleming, P. J.; Richards, F. M. *J. Mol. Biol.* **2000**, *299*, 487.
- (3) Klapper, M. H. *Biochim. Biophys. Acta, Protein Struct.* **1971**, *229*, 557.
- (4) Tsai, J.; Taylor, R.; Chothia, C.; Gerstein, M. *J. Mol. Biol.* **1999**, *290*, 253.
- (5) Wright, P. E.; Dyson, H. J. *J. Mol. Biol.* **1999**, *293*, 321.

- (6) Ptitsyn, O. B. *Curr. Opin. Struct. Biol.* **1995**, *5*, 74.
- (7) Petit, C. M.; Zhang, J.; Sapienza, P. J.; Fuentes, E. J.; Lee, A. L. *Proc. Natl. Acad. Sci. U. S. A.* **2009**, *106*, 18249.
- (8) Zhang, J.; Petit, C. M.; King, D. S.; Lee, A. L. *J. Biol. Chem.* **2011**, *286*, 41776.
- (9) Wand, A. J. *Curr. Opin. Struct. Biol.* **2013**, *23*, 75.
- (10) Igumenova, T. I.; Frederick, K. K.; Wand, A. J. *Chem. Rev.* **2006**, *106*, 1672.
- (11) Doyle, D. A.; Lee, A.; Lewis, J.; Kim, E.; Sheng, M.; MacKinnon, R. *Cell* **1996**, *85*, 1067.
- (12) Frauenfelder, H.; Hartmann, H.; Karplus, M.; Kuntz, I. D., Jr.; Kuriyan, J.; Parak, F.; Petsko, G. A.; Ringe, D.; Tilton, R. F., Jr. *Biochemistry* **1987**, *26*, 254.
- (13) Heerklotz, P. D. *Methods Mol. Biol.* **2007**, *400*, 197.
- (14) Fu, Y.; Kasinath, V.; Moorman, V. R.; Nucci, N. V.; Hilser, V. J.; Wand, A. J. *J. Am. Chem. Soc.* **2012**, *134*, 8543.
- (15) Frauenfelder, H.; Petsko, G. A.; Tsernoglou, D. *Nature* **1979**, *280*, 558.
- (16) Tilton, R. F., Jr.; Dewan, J. C.; Petsko, G. A. *Biochemistry* **1992**, *31*, 2469.
- (17) Fraser, J. S.; van den Bedem, H.; Samelson, A. J.; Lang, P. T.; Holton, J. M.; Echols, N.; Alber, T. *Proc. Natl. Acad. Sci. U. S. A.* **2011**, *108*, 16247.
- (18) Leitz, D.; Vogeli, B.; Greenwald, J.; Riek, R. *J. Phys. Chem. B* **2011**, *115*, 7648.
- (19) Gekko, K.; Obu, N.; Li, J.; Lee, J. C. *Biochemistry* **2004**, *43*, 3844.
- (20) Rouget, J. B.; Aksel, T.; Roche, J.; Saldana, J. L.; Garcia, A. E.; Barrick, D.; Royer, C. A. *J. Am. Chem. Soc.* **2011**, *133*, 6020.
- (21) Cooper, A. *Proc. Natl. Acad. Sci. U. S. A.* **1976**, *73*, 2740.
- (22) Wei, G.; Xi, W.; Nussinov, R.; Ma, B. *Chem. Rev.* **2016**, *116*, 6516.
- (23) Luong, T. Q.; Kapoor, S.; Winter, R. *ChemPhysChem* **2015**, *16*, 3555.
- (24) Dellarole, M.; Caro, J. A.; Roche, J.; Fossat, M.; Barthe, P.; Garcia-Moreno, E. B.; Royer, C. A.; Roumestand, C. *J. Am. Chem. Soc.* **2015**, *137*, 7354.
- (25) Neumaier, S.; Buttner, M.; Bachmann, A.; Kiefhaber, T. *Proc. Natl. Acad. Sci. U. S. A.* **2013**, *110*, 20988.
- (26) Motlagh, H. N.; Wrabl, J. O.; Li, J.; Hilser, V. J. *Nature* **2014**, *508*, 331.
- (27) Jackson, S. E. *Folding Des.* **1998**, *3*, R81.
- (28) Pace, C. N.; Shaw, K. L. *Proteins: Struct., Funct., Genet.* **2000**, *Suppl 4*, 1.
- (29) Acharya, N.; Mishra, P.; Jha, S. K. *J. Phys. Chem. Lett.* **2016**, *7*, 173.